The Journal of Neuroscience, November 1, 1996, *16*(21):6676–6686

Axonal Action-Potential Initiation and Na^+ Channel Densities in the Soma and Axon Initial Segment of Subicular Pyramidal Neurons

Costa M. Colbert and Daniel Johnston

Division of Neuroscience, Baylor College of Medicine, Houston, Texas 77030

A long-standing hypothesis is that action potentials initiate first in the axon hillock/initial segment (AH–IS) region because of a locally high density of Na^+ channels. We tested this idea in subicular pyramidal neurons by using patch-clamp recordings in hippocampal slices. Simultaneous recordings from the soma and IS confirmed that orthodromic action potentials initiated in the axon and then invaded the soma. However, blocking Na^+ channels in the AH–IS with locally applied tetrodotoxin (TTX) did not raise the somatic threshold membrane potential for orthodromic spikes. TTX applied to the axon beyond the AH–IS (30–60 μm from the soma) raised the apparent somatic threshold by ~8 mV. We estimated the Na^+ current density in the AH–IS and somatic membranes by using cell-attached patch-clamp recordings and found similar magnitudes (3–4 pA/μm^2). Thus, the present results suggest that orthodromic action potentials initiate in the axon beyond the AH–IS and that the minimum threshold for spike initiation of the neuron is not determined by a high density of Na^+ channels in the AH–IS region.

Key words: action potential; action-potential initiation; Na^+ channel; patch-clamp recording; hippocampus; pyramidal neuron; single-channel recording; dual-electrode recording

An important aspect of neuronal integration is the transformation of information in the form of membrane potential to all-or-none action potentials for communicating with other cells and for signaling within the dendritic tree of the neuron. Where this conversion occurs in the neuron has important implications for the function of a neuron (Levy et al., 1990; Jaslove, 1992; Softky and Koch, 1993; Shadlen and Newsome, 1994). Classic work on the motoneuron (Araki and Otani, 1955; Coombs et al., 1957; Fuortes et al., 1957) suggested that action potentials initiate in the initial segment/axon hillock region of the neuron, presumably because of a more negative transmembrane potential threshold for action-potential initiation in this region than in the soma. Although the site of initiation under all conditions is not completely resolved in cells with active dendrites (Adams, 1992; Johnston et al., 1996), much recent evidence from pyramidal and other neurons supports the classical notion that action potentials initiate first in the axon and then propagate into the soma and dendrites (Turner et al., 1991; Jaffe et al., 1992; Stuart and Sakmann, 1994; Häusser et al., 1995; Spruston et al., 1995).

Why would the action potential initiate first in the initial segment? Dodge and Cooley (1973) suggested that a high local density of Na^+ channels would lower the threshold membrane potential, speculating a density as high as in the nodes of Ranvier. Indeed, electron microscopists had identified membrane similarities between the initial segment and the nodes (Palay et al., 1968; Peters et al., 1968). Later modeling studies provided theoretical justification for such a high density, making strong predictions about the overall firing threshold of the neuron and the ability to backpropagate an action potential into the soma (Moore et al., 1983; Traub et al., 1994; Mainen et al., 1995).

We wished to test the hypothesis that a high local density of Na^+ channels in the initial segment determines the minimum threshold of the neuron for action-potential initiation. Using video-enhanced differential interference (DIC) microscopy in brain slices (Stuart et al., 1993), we identified somata and initial segments of subicular pyramidal neurons. We recorded Na^+ currents from these structures by using cell-attached patch-clamp techniques and, to our surprise, found no large regional difference in Na^+ channel density. Thus, we recorded simultaneously from initial segments and somata, verifying that orthodromic action potentials initiate in the axon. Finally, as a first step in determining the mechanisms of axonal initiation, we explored the relationship between local Na^+ channel density and the lowest threshold of the neuron for action-potential initiation. By locally applying tetrodotoxin (TTX) to block Na^+ channels, we found that Na^+ channels in the axon, but not in the initial segment, determine the minimum threshold for action-potential initiation. Thus, the results suggested that action potentials initiate in the axon at some distance from the soma and that the local density of Na^+ channels in the axon hillock/initial segment, which is not high, does not determine the lowest threshold of the neuron for action-potential initiation.

MATERIALS AND METHODS

Preparation and solutions. The present study used 2- to 8-week-old Sprague Dawley rats of both sexes. Older animals were anesthetized with a lethal dose of a combination of ketamine, xylazine, and acepromazine. Once deeply anesthetized, they were perfused through the heart with cold modified artificial cerebrospinal fluid (ACSF) containing (in mM): 124 NaCl, 2.5 KCl, 1.2 NaH_2PO_4, 25 $NaHCO_3$, 0.5 $CaCl_2$, 7.0 $MgCl_2$, and 20 dextrose and bubbled with 95%O_2/5%CO_2. In some animals, 110 mM choline chloride was substituted for NaCl. This procedure aided visualization during recording and decreased background blood vessel staining in slices prepared for neuron reconstructions. Young pups were decapitated consciously. After removal of the brain, 300- to 400-μm-thick slices

Received June 19, 1996; revised Aug. 5, 1996; accepted Aug. 12, 1996.

This work was supported by National Institute of Mental Health Grants MH10896 to C.M.C. and NS11535, MH44754, and MH48432 to D.J.

We thank Jeffrey Magee for helpful discussions throughout this study, Janet Stringer for comments on an earlier version of this manuscript and for help performing the biocytin experiments, and Tamas Freund for suggesting the anatomical method for estimating the length of the initial segment.

Correspondence should be addressed to Costa M. Colbert, Division of Neuroscience, Baylor College of Medicine, One Baylor Plaza, Houston, TX 77030.

were cut using a Vibratome (Lancer), incubated submerged in a holding chamber for 30 min at 32°C, and stored submerged at room temperature. Except where otherwise noted, all recordings were made submerged at room temperature (~24°C in bath). During the slicing procedure, the slices were maintained in the same ACSF as used for the perfusion. The holding chamber solution contained (in mM): 120 sucrose, 64 NaCl, 2.5 KCl, 1.2 NaH_2PO_4, 25 $NaHCO_3$, 1.5 $CaCl_2$, 3.5 $MgCl_2$, and 20 dextrose and was bubbled with 95%O_2/5%CO_2. The external recording solution contained 124 NaCl, 2.5 KCl, 1.2 NaH_2PO_4, 25 $NaHCO_3$, 2.0 $CaCl_2$, 1.0 $MgCl_2$, and 20 dextrose and was bubbled with 95%O_2/5%CO_2. In experiments where antidromic stimuli were delivered, kynurenic acid (5–10 mM, Sigma, St. Louis, MO) was added to the external solution to block synaptic activation evoked by the stimulus. The internal pipette solution used for whole-cell recordings contained (in mM): 120 K-gluconate, 20 KCl, 10 HEPES, 0.4 EGTA, 4.0 NaCl, 4.0 MgATP, 0.3 MgGTP, and 14 phosphocreatine adjusted to pH 7.25 with KOH. The internal pipette solution for cell-attached patch recordings contained (in mM): 120 NaCl, 30 tetraethylammonium chloride, 10 HEPES, 2 $CaCl_2$, 3 KCl, 1 $MgCl_2$, and 5 4-aminopyridine (4-AP) adjusted to pH 7.4 with NaOH. $CdCl_2$ (200 μM) was included in the solution in approximately one-third of the pipettes.

Recording techniques. Recordings were made from somata and initial segments of subicular pyramids just beyond the end of the hippocampal CA1 cell layer in horizontal hippocampal slices. Neurons were visualized using infrared differential interference contrast (DIC) optics (Axioskop, Ziess, Oberkochen, Germany) according to standard techniques (Stuart et al., 1993). Patch-clamp recordings in the whole-cell mode were made using a microelectrode amplifier (Axoclamp 2A, Axon Instruments, Foster City, CA) using pipettes (3–5 MΩ) of borosilicate glass (Drummond, Broomall, PA) coated with SYLGARD (Dow Corning, Corning, NY) and pulled using a P-87 Flaming–Brown pipette puller (Sutter Instruments, Novato, CA). Cell-attached patch recordings were made using a patch-clamp amplifier with a capacitive headstage (Axopatch 200A, Axon Instruments). The same pipette glass was used as in the whole-cell recordings, but the pipettes had much smaller tips (~0.5 μm, 8–10 MΩ; see Fig. 1*A*). Whole-cell recordings were low-pass-filtered at 3 kHz (6 dB/octave) and digitized at 10 kHz except when the shape of the action potential was observed. In these cases, a low-pass filter of 10 kHz and a sampling rate of 50 kHz was used. Cell-attached patch recordings were filtered at 2 kHz (8-pole Bessel filter) and sampled at 10 kHz. Data were digitized at 16 bit resolution (ADC488/16, IOTech) and stored by computer for off-line analysis (Next Computer). Antidromic action potentials were stimulated by constant current pulses (Neurolog, Digitimer) through a monopolar tungsten electrode (AM Systems) placed in the alveus.

Identification of axons. Subicular pyramidal cells were chosen over CA1 pyramids because the somata do not lie in a tight cell layer. The tight packing of CA1 somata made visualization of the relatively small axon initial segments (<2 μm in diameter) difficult. Furthermore, many CA1 axons begin on basal dendrites rather than on the soma. In DIC, the initial segment membrane appeared as an extension of the somatic membrane and was the only basal structure easily seen without cleaning. Basal dendrites were typically more difficult to visualize until a pipette with positive backpressure was lowered into the region of the initial segment, which had somewhat of a cleaning action. In cells that we have found to be less healthy on the basis of resting membrane potential and input resistance, basal dendrites could not be distinguished clearly from the axon because of a generalized increase in the contrast of the cell. We chose only pyramidal cells that seemed to have only a single branch coming from the soma approximately opposite and parallel to the apical dendrite. To verify that our visual criteria could be used effectively to identify axons, we filled the neurons with biocytin, using a second recording pipette in whole-cell mode (Horikawa and Armstrong, 1988) after the cell-attached path recordings were complete ($n = 14$). A video image of the soma and initial segment was digitized and stored for later comparison (see Fig. 1*A*). Slices were fixed in 4% paraformaldehyde in phosphate buffer solution (0.1M, pH 7.4), and the biocytin-filled neurons were visualized using avidin-biotinylated horseradish peroxidase (Vectastain ABC kit, Vector Labs, Burlingame, CA) complexed with 3,3′-diaminobenzidine tetrahydrochloride (DAB kit, Vector Labs). All of the filled cells were pyramidal in morphology, and axons were identified by following their path to the alveus. Camera lucida drawings (see Fig. 1*B*) were made from video images taken at various focal planes and rechecked in the microscope. Not all structures that we assumed to be axons could be followed to the alveus but, instead, came to an end at the surface of the slice. In such cases, there was never another structure that reached the alveus. In all cells where the axon could be positively identified, we had identified the axon correctly. Thus, we are confident that the great majority of the patch recordings was indeed made on initial segments.

Unfortunately, no definitive measure of the extent of the initial segment exists to date for subicular pyramidal neurons. Thus, we attempted to determine the length of the unmyelinated initial segment by a modification of the extracellular biocytin technique (King et al., 1989) suggested to us by Tamas Freund (personal communication). By processing the tissue without detergent or freezing, myelinated axons show greatly decreased staining, because the reagents must cross the multiple lipid bilayers. We made three injections of biocytin (4%, 1.5 μl at each location) in each subiculum of urethane-anesthetized rats (200 gm; $n = 2$). Coordinates were (in mm) from lambda [1.5 anterior–posterior (AP), 2.5 medial–lateral (ML), −2.5 dorsal–lateral (DV) and 1.0 AP, 4.5 ML, −3.5 DV] and from bregma (−3.5 AP, 1.0 ML, −3.0 DV). Bite bar was at 0 mm. After survival times of 5 and 12 hr, the rats were deeply anesthetized and then transcardially perfused with 0.9% saline, followed by 10% formalin and 4% paraformaldehyde. Coronal sections, 50 or 100 μm thick, were cut by a vibratome. Sections were processed alternately with and without detergent. In the sections processed with detergent, many stained fibers could be seen in the alveus and in the terminal zones of the perforant path. Much less staining of the alveus was seen in the sections processed without detergent. Using the same criteria for choosing cells and initial segments as described above, we identified initial segments and measured their lengths (19.9 ± 0.75 μm; mean ± SEM, range 15–30 μm; $n = 34$). Beyond this length, staining of the axon was either not visible or just faintly visible as a hairline. Axons beyond the initial segment in sections processed with detergent, on the other hand, were more darkly stained and could often be followed to the alveus. Although this method is not unequivocal because of limitations on identifying axons, possible variations in thickness of the myelin, et cetera, the results suggest that the axons of the subicular pyramidal neurons are myelinated beyond an initial segment of ~20 μm. These results seem consistent with the electron microscopic data of Farinas and DeFelipe (1991) in cortical pyramidal neurons and with the extent of axoaxonic contacts on the proximal axon of subicular pyramids (Somogyi et al., 1982).

RESULTS

Estimates of sodium channel densities in initial segment and soma

To test the hypothesis that the density of Na^+ channels in the initial segment is greater than that in the soma, we directly measured Na^+ currents through the initial segment and somatic membranes by using cell-attached patch-clamp techniques (Stuart et al., 1993; Magee and Johnston, 1995b). Axon initial segments were identified for recording based on morphology as visualized, using DIC optics (Fig. 1*A*). Neurons were subsequently filled with biocytin and reconstructed so that an unequivocal identification of the axon could be made (Fig. 1*B*; see Materials and Methods). As a test that we were indeed recording from the pyramidal cell axon and not some other cell (e.g., glia), we ruptured the patch immediately after making the seal in five consecutive cells. An action potential could always be recorded. At the end of each patch recording, we attempted to break into the cell to establish the resting potential and to verify that an action potential could be evoked. In approximately one-fourth of the patches we were unsuccessful in gaining access to the cell.

Na^+ channel activity in cell-attached patches was identified as fast inward current with voltage-dependent kinetics. Depolarizing steps from a holding potential of −90 mV to a command potential of approximately −10 mV yielded synchronous activation of the Na^+ channels in the patch (Fig. 2*A*). Smaller depolarizing steps (approximately −30 to −40 mV) evoked less synchronous initial activation. In some trials, currents from additional openings could be seen throughout the duration of the 50 msec command potential (more probable in the smaller depolarizations; Fig. 2*A*). The amplitudes of these currents were equal to or were small multiples

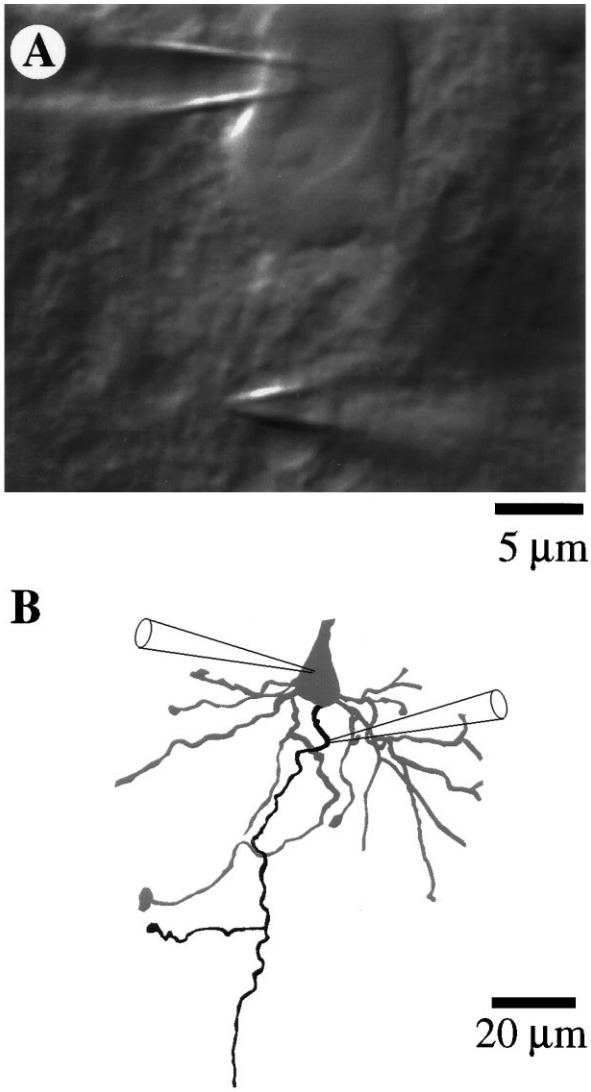

Figure 1. Whole-cell patch and cell-attached patch recordings from subicular pyramidal cells. *A*, Differential interference contrast (DIC) image of soma and initial segment showing the positions of the whole-cell somatic recording electrode (*upper right*) and the cell-attached initial segment recording electrode (*lower right*). *B*, Morphological reconstruction of soma and basal portion of the cell after biocytin filling and subsequent visualization. The identity of the axon (*black process*) was verified by following its path into the alveus. Cell 95066b.

of a unitary current amplitude (i.e., current through a single open Na^+ channel). Plotting the unitary current amplitude versus command potential ($n = 7$; Fig. 2*B*) yielded a slope conductance of 14.8 pS and an extrapolated Na^+ reversal potential of +58 mV. Mg^{2+} (1 mM; $n = 5$) or Cd^{2+} (0.2 mM; $n = 5$) had no apparent effect on channel activity.

Comparisons of Na^+ current density between cell-attached patches on the soma ($n = 20$) and patches on the initial segment (3–30 μm from the soma; $n = 27$) were made using similar pipettes. Peak current was the maximum amplitude seen in 30–50 depolarizing steps to approximately −10 mV (Fig. 2*A*), and was normalized for the area of the patch estimated visually. The initial 10 somatic recordings were divided into two groups based on site: either central somatic or axon hillock. Axon hillock sites were defined as those within 3 μm from the site of attachment of the axon. No significant difference in peak current was seen between the central somatic (3.29 ± 0.45 pA/μm^2; $n = 5$) and axon hillock sites (3.08 ± 0.51 pA/μm^2; $n = 5$). The remaining somatic recordings were made from the central somatic region. Although there was some variability between patches, the peak current per area did not increase as a function of distance from the soma ($m = 0.09$; $r^2 = 0.17$; Fig. 2*C*). For comparison of the somatic and initial segment peak currents, the animals were divided into two groups based on age: pups ~2 weeks and older rats from 4–8 weeks. In the younger age group, the peak current density in the soma was 2.9 ± 0.36 pA/μm^2 (mean ± SEM; $n = 10$), and in the initial segment it was 2.87 ± 0.33 ($n = 18$). In the older age group, the peak current density in the soma was 3.2 ± 0.47 pA/μm^2 ($n = 10$) and in the initial segment it was 4.0 ± 0.35 pA/μm^2 ($n = 9$). To convert from peak current density to the density of Na^+ channels in the membrane, we assumed that the peak current represents synchronous opening of all the Na^+ channels in the patch. Thus, the number of channels in the patch was the peak current divided by the unitary current amplitude (current through a single open Na^+ channel). From the *I–V* plot (Fig. 2*B*), the unitary current amplitude was ~1 pA at −10 mV. Thus, assuming an opening probability of one at −10 mV and an accurate estimate of the patch area, the density of Na^+ channels was three to four channels per micrometer squared throughout the somatic and initial segment membrane.

The results of these measurements did not support the hypothesis of a very high density of Na^+ channels in the initial segment/axon hillock region. Thus, we tested a number of hypotheses related to the site of action-potential initiation, the sequence of Na^+ channel activation as the action potential invades the soma, and the relative thresholds for the initiation of action potentials in the axon and soma.

Sequence of action-potential invasion of the soma

We determined the sequence of invasion of the action potential into the initial segment and soma by recording simultaneously from these structures (Fig. 1). Axon initial segments were identified as above using DIC optics (Fig. 1*A*; see Materials and Methods). Current-clamp recordings from the soma were made in the whole-cell configuration (Fig. 3; *Soma* V_m; $n = 5$). The temporal derivative of the membrane potential (Fig. 3; *Soma* dV_m/dt) was calculated to increase the resolution of individual components of the action potential (Coombs et al., 1957). Recordings from the initial segment were made in cell-attached mode in voltage clamp. The transmembrane potential was held near 0 mV to inactivate Na^+ channels in the patch. Thus, the cell-attached electrode recorded capacitive transients across the membrane (Fig. 3; *IS patch*), which were proportional to the temporal derivative of the membrane potential (Magee and Johnston, 1995a). A comparison of whole-cell and cell-attached recordings from adjacent sites on the soma verified that this technique worked as expected (data not shown).

To test the hypothesis that orthodromic action potentials initiate somewhere in the axon and then propagate back into the soma, we compared the sequence of charging of the initial segment and soma in response to antidromic and orthodromic stimulation. If orthodromic action potentials are actually initiated in the axon, then the sequence of charging should be the same for both antidromic and orthodromic action potentials. Recording simultaneously in the initial segment (IS) and soma, antidromic action potentials were evoked by single shocks in the alveus (Fig. 3, *left* panel; *IS patch* ~10 μm from soma). The action potential recorded in the soma (Figure 3; *Soma* V_m) had a rising phase with

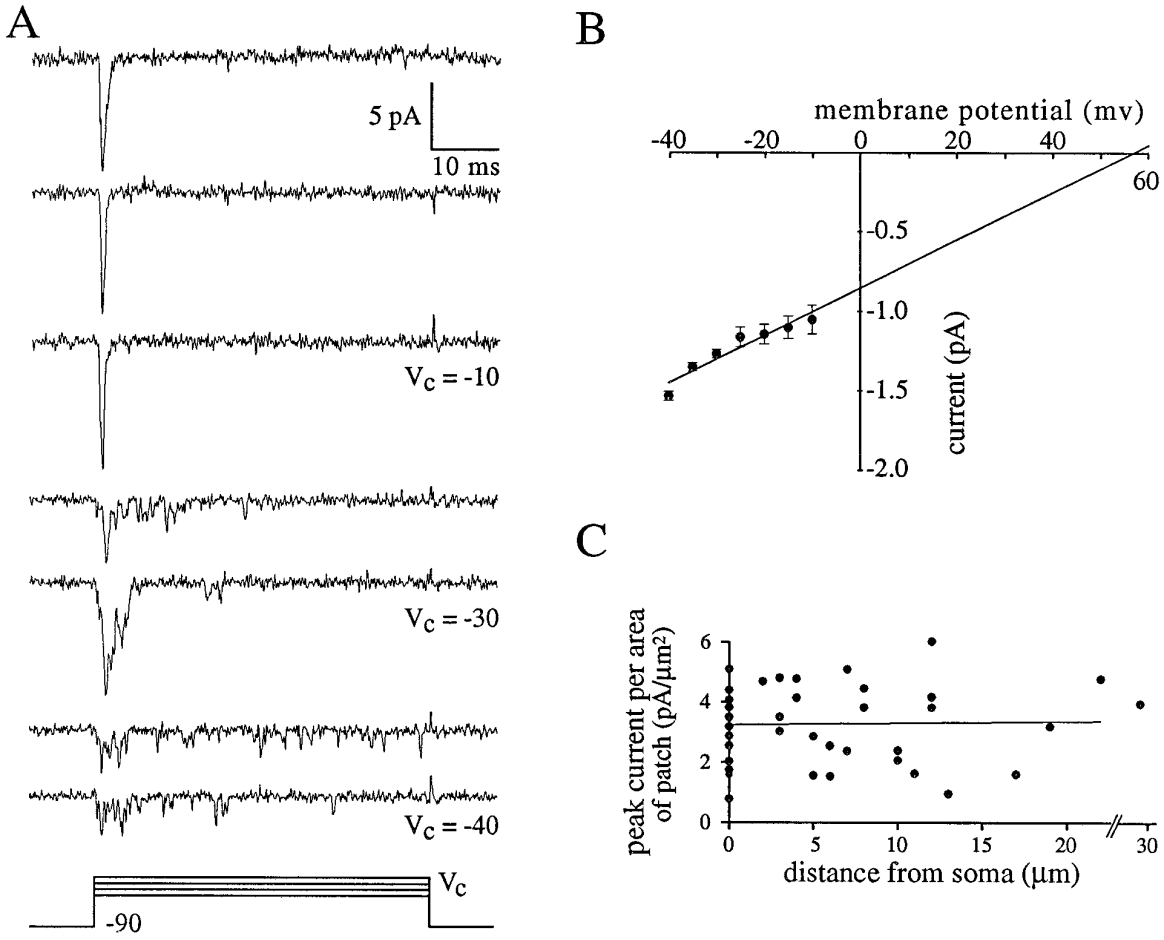

Figure 2. Cell-attached recordings from axon initial segment. *A*, Na^+ channel activity after depolarizing steps from −90 to −10, −30, and −40 mV. *Traces* are individual consecutive sweeps. Note single channel openings throughout the steps to −40 mV. Cell c95064. *B, I–V* plot of Na^+ channel activity. Unitary current amplitudes are plotted as a function of membrane potential. The linear regression crosses the membrane potential axis at +58 mV and has a slope of 14.8 pS. Error bars are SEM. *C*, Summary of peak Na^+ currents in cell-attached patches from initial segment (n = 27) and soma (n = 20). Peak current per area of patch (pA/μm^2) is plotted as a function of the distance of the patch from the soma. The points at zero distance correspond to somatic patches. The linear regression line through all points has a slope of 0.018 pA/μm^2 per micrometer from soma.

two distinct components, corresponding to two peaks, P1 and P2, in the derivative (Figure 3; *Soma* dV_m/dt). P1 was always small relative to P2 in the somatic recordings. The two peaks also appeared in the recording from the initial segment (Fig. 3; *IS patch*), but compared with the peaks in the somatic waveform, P1 was much larger relative to P2. This difference in relative magnitude of the peaks corresponds to a much greater initial rate of rise of the initial segment membrane potential as compared with the somatic membrane potential. The slower rate of charging of the soma is consistent with its greater capacitance. These data suggest the following interpretation for the sequence of invasion of an antidromic action potential, which is essentially that of Coombs et al. (1957). The initial peak (*P1*) represents the change in membrane potential attributable to the action potential actively invading the initial segment (i.e., activating Na^+ channels in the initial segment) and passively charging the soma. The second peak (*P2*) represents activation of Na^+ channels in the soma and dendrites, which the initial segment follows passively.

As a test of the hypothesis that the peaks represented charging attributable to distinct events (i.e., activation of Na^+ channels in the initial segment vs the soma), we dissociated the appearance of the peaks. Two antidromic action potentials were evoked at a latency during the relative refractory period of the soma that produced some failures of the full somatic action potential (Fig. 3, *right* panel; *Soma* V_m). When the soma fired (in 2 of 4 pairs of stimuli), the action potential was delayed, as were the P2 peaks (Fig. 3; *IS patch*). When failures occurred, only a single peak was detected in the initial segment [Fig. 3; *IS patch* (*failures*)]. Throughout, the P2 peaks in the initial segment correlated well in magnitude and latency with the somatic P2 peaks. The P1 peak was independent of the presence of a somatic action potential and did not vary in latency (Fig. 3, *right* panel). Thus, the existence of two peaks in the waveforms seems to result from distinct activation of channels in the initial segment and soma.

With the sequence of invasion determined for the antidromic action potential, we observed the sequence of invasion of orthodromic action potentials in the same recording configuration (Fig. 4*A*). The orthodromic stimulus was a current injection through the somatic electrode. The orthodromic action potentials produced a similar pattern of peaks in the recordings from the soma and initial segment, although the latency between the peaks was reduced (Fig. 4*B; Soma* dV_m/dt, *IS patch*). The shorter latency would be expected because the orthodromic stimulus partially charged the capacitance of the soma before initiation of an action

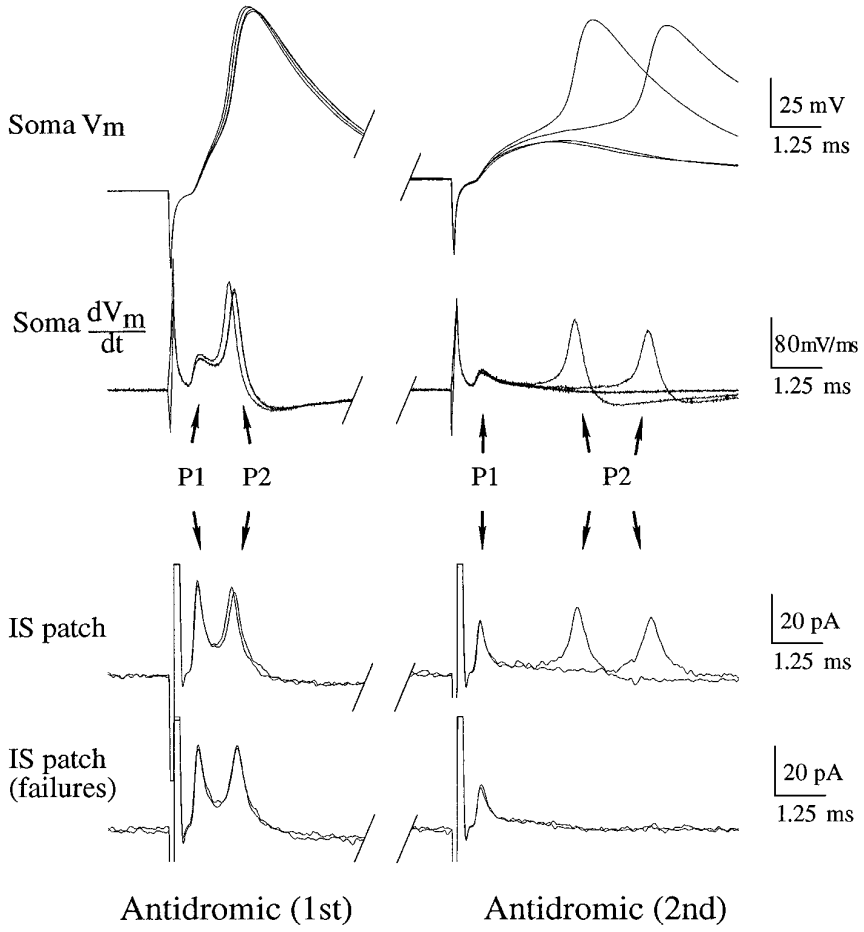

Figure 3. Sequence of antidromic action-potential (AP) invasion of initial segment (*IS*) and soma. Dual-recording electrode positions are as in Figure 1. Waveforms are individual sweeps. *Antidromic (1st), Left column* shows response to a single antidromic AP. *Antidromic (2nd), Right column* is the response to the second of a pair of antidromic APs. *Soma* V_m, Membrane potential recorded through the somatic whole-cell electrode. *Soma* dV_m/dt, Time derivative of the somatic membrane potential. *IS patch*, Cell-attached patch recording in the IS. The current recorded is primarily capacitive and, thus, is proportional to the time derivative of the transmembrane potential of the patch. *IS patch (failures)*, Cell-attached recordings in the IS, in which the second antidromic action potential failed to invade the soma. *P1* corresponds to the peak in the response attributable to charging of the patch by channels in the IS. *P2* corresponds to the charging of the patch by somatic Na^+ channels, which does not occur when the second somatic AP fails. See text for details. RMP, −63 mV. Cell c95066a.

potential. Thus, when the action potential backpropagated from the initial segment into the soma, the current from the initial segment could activate somatic Na^+ channels more rapidly. A similar argument could be made for the greater latency of the peaks corresponding to the second action potential (Fig. 3*B; Soma* dV_m/dt*, IS patch*). Presumably, because the second action potential initiated during the relative refractory period after the first action potential, charging of the soma was somewhat slower during the somatic invasion of the second action potential, activation of somatic Na^+ channels was delayed, and, thus, the interval between the peaks was increased. The data from these dual recordings suggested that the sequence of charging of the initial segment and the soma is the same. Thus, under the conditions of our preparation and with our using a current step through the somatic electrode as the orthodromic stimulus, action potentials initiated in the axon before the soma.

Alterations of action-potential initiation by local TTX application

We used the following rationale to examine the relationship between local Na^+ channel density and the site of initiation of action potentials. Although the threshold for action-potential initiation depends on many factors, including local morphology and the relative magnitude of inward and outward voltage-gated conductances, decreasing functional Na^+ channel density should raise threshold. If there is a region of the cell with a particularly low threshold (for any reason, not just because of high Na^+ channel density), then decreasing the inward Na^+ current in this region should increase the local threshold and, thus, the overall threshold of the cell. On the other hand, decreasing the Na^+ channel density in some other region of the cell (i.e., one that does not have the lowest threshold), will have less effect on the overall threshold of the cell, because the site with the lowest threshold will still fire at its (lower) threshold. Using this rationale, we blocked Na^+ channels locally in the axon, initial segment, soma, and dendrites to test if one region had a particularly low threshold as implied by Coombs et al. (1957). We also tested the hypothesis of Mainen et al. (1995) that Na^+ channels in the initial segment provide most of the conductance underlying the somatic action potential.

The remainder of the experiments used a single somatic patch-clamp electrode in whole-cell mode to record somatic action potentials. Tetrodotoxin (TTX, 10 μM) was ejected from a small patch pipette (tip, <1 μm in diameter) onto different parts of the cell to block Na^+ channels. The slice was positioned so that the flow of the external medium was away from the soma toward the alveus. In all cases the initial segment was identified, and the ejection of TTX was confirmed visually. To assess the effect of TTX on action-potential initiation, we sequentially stimulated the cell orthodromically and then antidromically within a single sweep. A single shock from a stimulating electrode in the alveus activated antidromic action potentials. A depolarizing current step through the somatic recording electrode evoked orthodromic action potentials. An interval of 100 msec between stimuli within each sweep was sufficiently long enough to prevent interaction of the stimuli but short enough to maintain a relatively constant concentration of TTX during the pair of stimuli. Altering the

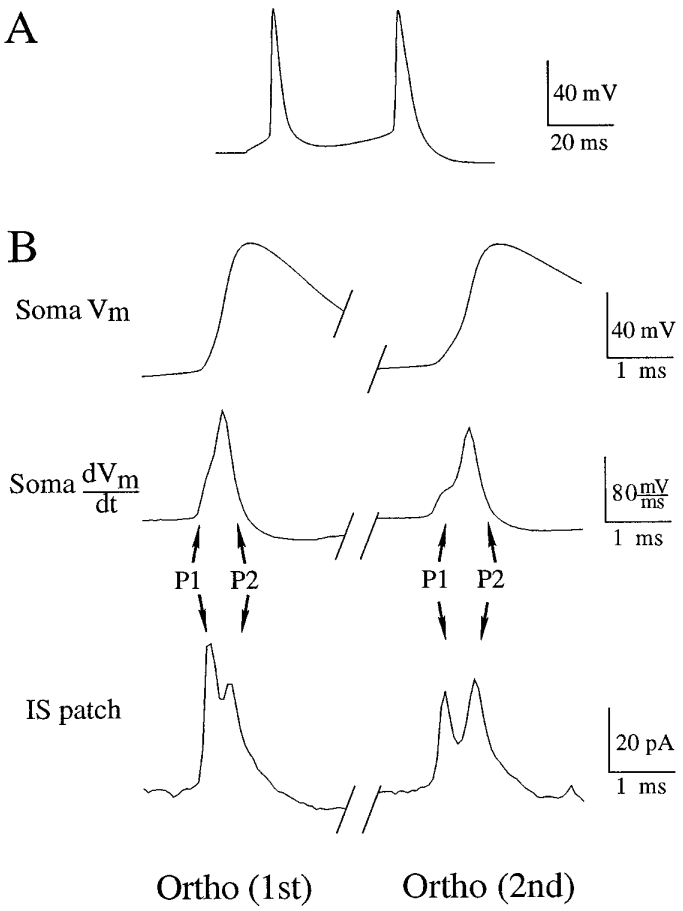

Figure 4. Sequence of orthodromic action-potential (AP) invasion of initial segment (*IS*) and soma. Dual-recording electrode positions are as in Figure 1. Waveforms are single sweeps. *A*, Somatic membrane potential recorded through the whole-cell electrode. Orthodromic action potentials were evoked by a 50 msec duration, 200 pA current injection through the recording electrode. *B, Ortho (1st), Left column* corresponds to the first action potential evoked by the orthodromic stimulus. *Ortho (2nd), Right column* corresponds to the second action potential initiated by the stimulus. *Soma* V_m, Membrane potential recorded through the somatic whole-cell electrode. *Soma* dV_m/dt, Time derivative of the somatic membrane potential. *IS patch*, Cell-attached patch recording in the IS. The current recorded is primarily capacitive and, thus, is proportional to the time derivative of the transmembrane potential of the patch. *P1* and *P2* correspond to charging of the patch by channels in the initial segment and soma, respectively, as in Figure 3. Note that, although the peaks occur with shorter latency, the sequence of invasion of orthodromic APs is the same as that for antidromic APs. Cell c95066a.

order of the stimuli or the durations of the current injections (data not shown) did not yield results different from those presented here.

Initially, the effect of TTX on the initial segment was tested by locally applying TTX 10–15 μm from the soma in small volumes (n = 8; Fig. 5*A*). During the application of TTX, the orthodromic current step continued to fire full action potentials of similar amplitude at similar latency and somatic membrane potential. The antidromic action potential, however, failed as it invaded the soma, leaving a partial action potential ~25 mV in amplitude (Fig. 5*B, arrow*). This result might be explained in two ways. First, there could be a similar threshold in the soma and initial segment so that blocking the initial segment does not greatly alter the threshold in the soma in response to depolarization. Second, the orthodromic depolarization could summate with the (now re-

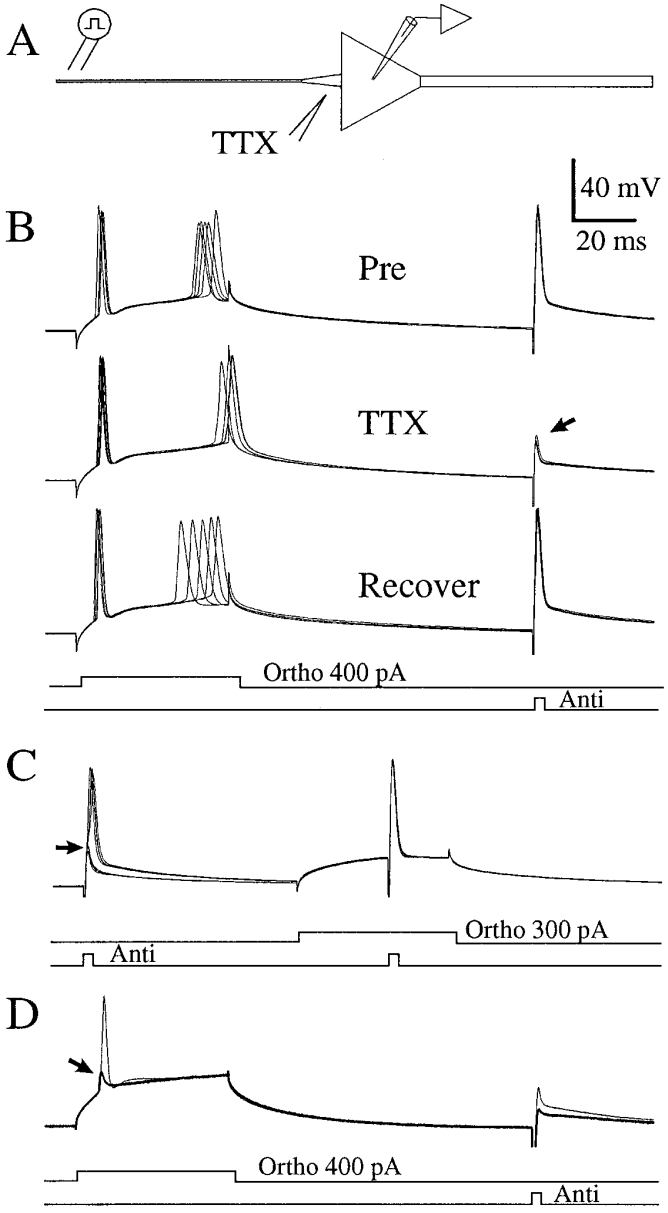

Figure 5. Local application of TTX to the initial segment (IS) impairs antidromic invasion of the soma without significantly altering the threshold for orthodromic AP initiation. *A*, A somatic whole-cell electrode recorded from an injected current into the soma. A stimulating electrode in the alveus evoked antidromic APs. TTX was applied to the IS (12 μm from the soma). *B, Traces* are somatic whole-cell current-clamp records of the response to orthodromic and antidromic APs. *Pre*, Six consecutive baseline sweeps. *TTX*, Six consecutive sweeps during TTX application. Note that the antidromic AP failed to invade the soma (*arrow*), but the orthodromic AP initiated with similar latency and membrane-potential threshold. *Recover*, Five consecutive sweeps as the cell recovered. *C*, The full somatic AP was not mediated by Na^+ channels in the IS but by somatic Na^+ channels. Sweeps with and without TTX are superimposed. In the presence of TTX, the antidromic AP failed to invade the soma (*arrow*). Pairing subthreshold depolarization with an antidromic AP allowed the soma to fire a full AP. Note that the paired antidromic AP in TTX was indistinguishable from the control condition. Thus, somatic channels were sufficient to produce a full AP. RMP, −63 mV. *D*, In another cell, a greater ejection of TTX decreased the amplitude of the antidromic AP to ~10 mV (*bold trace*). The orthodromic stimulus evoked a similar small spike (*arrow*) that was insufficient to fire the soma but had the same latency and threshold as APs before the application of TTX. The following sweep (*thin trace*) had a somewhat larger antidromic AP (25 mV). This greater current from the IS, paired with the depolarization of the soma by the orthodromic stimulus, resulted in a full somatic AP. RMP, −65 mV. Cell c95082.

duced) current from the backpropagating action potential sufficiently to activate somatic Na^+ channels and fire the cell. To distinguish between these possibilities, we paired subthreshold depolarization of the soma with an antidromic action potential (Fig. 5*C; n* = 4). Two antidromic stimuli were given at a latency of 100 msec. The second stimulus in the sweep was paired with a subthreshold depolarization of the soma. The unpaired antidromic action potentials failed when TTX was applied to the initial segment (Fig. 5*C, arrow*), but the antidromic action potentials paired with depolarization produced somatic action potentials that were indistinguishable from the pre-TTX controls. Thus, action potentials initiated in the axon in response to a somatic current injection could indeed summate with somatic depolarization to fire a full somatic action potential. To test this idea further, we repeated the paradigm of Figure 5*B* with a larger volume of TTX ejected from the pipette to decrease the amplitude of the spikes propagating from the axon to the soma (*n* = 4). When the antidromic action potential was made very small (10–15 mV; Fig. 5*D, bold trace*), the orthodromic action potential also failed (Fig. 5*D, arrow*), consistent with the idea that orthodromic spikes were initiated in the axon. As the cell began to recover from the TTX, as indicated by the larger antidromic action-potential amplitude, a full action potential followed the orthodromic stimulus (Fig. 5*D, thin trace*).

Despite its profound effects on the ability of the action potential to invade the soma, the application of TTX to the initial segment did not greatly alter the latency or the somatic membrane potential at which the action potentials appeared. Thus, according to the argument outlined above, the initial segment was not the site of initiation of action potentials. Furthermore, although Na^+ channels in the initial segment supplied current to charge the soma during the somatic invasion of the action potential, somatic Na^+ channels, once activated, were of sufficient density to produce a full action potential in the soma. To refine this result further, we applied TTX locally to the soma and to the proximal apical dendrite of the pyramidal neurons (Fig. 6*A*; *n* = 6).

Application of TTX regions near the soma resulted in distinct patterns of invasion of the action potential in single cells (Fig. 6; *n* = 5). TTX applied to the initial segment in small volumes, as before, reduced the antidromic action potential without altering the orthodromic action potential (Fig. 6*B, bold trace*). TTX applied to the soma altered both the orthodromic action potential and the antidromic action potential (Fig. 6*C*). At the peak of the effect of TTX application to the soma, the orthodromic action potential initiated at a similar membrane potential as in the control condition (*filled arrow*, thin trace) but was delayed, broad, and reduced in amplitude (Fig. 6*C* and *inset; filled arrow, bold traces*). Because larger ejection volumes of TTX were used at the soma, some TTX likely diffused to the initial segment, which itself would explain the failure of the antidromic action potential to invade the soma. The reduced amplitude of the somatic action potential, however, was not explained simply by decreased current from the initial segment: when TTX was applied to the soma (Fig. 6*C*), the failed antidromic action potential, which provided a measure of the current flow from the axon into the soma, was actually slightly larger than when TTX was applied to the initial segment (Fig. 6*B*). These results support the notion that activation of somatic Na^+ channels is not only sufficient to produce a full action potential in the soma, but necessary. Finally, applying TTX to the very proximal apical dendrite had no effect (Fig. 6*D*), even when relatively large ejection volumes were used, as compared with those applied to the initial segment. Thus, there was no evidence for dendritic involvement in the initiation of action potentials in response to the orthodromic stimuli used (i.e., current injection at the soma). TTX applied to regions of the cell near the soma had little effect on the somatic membrane potential at which orthodromic action potentials appeared at the soma. Thus, for the orthodromic stimuli used, the site of initiation was not in the soma, initial segment, or the proximal dendrite.

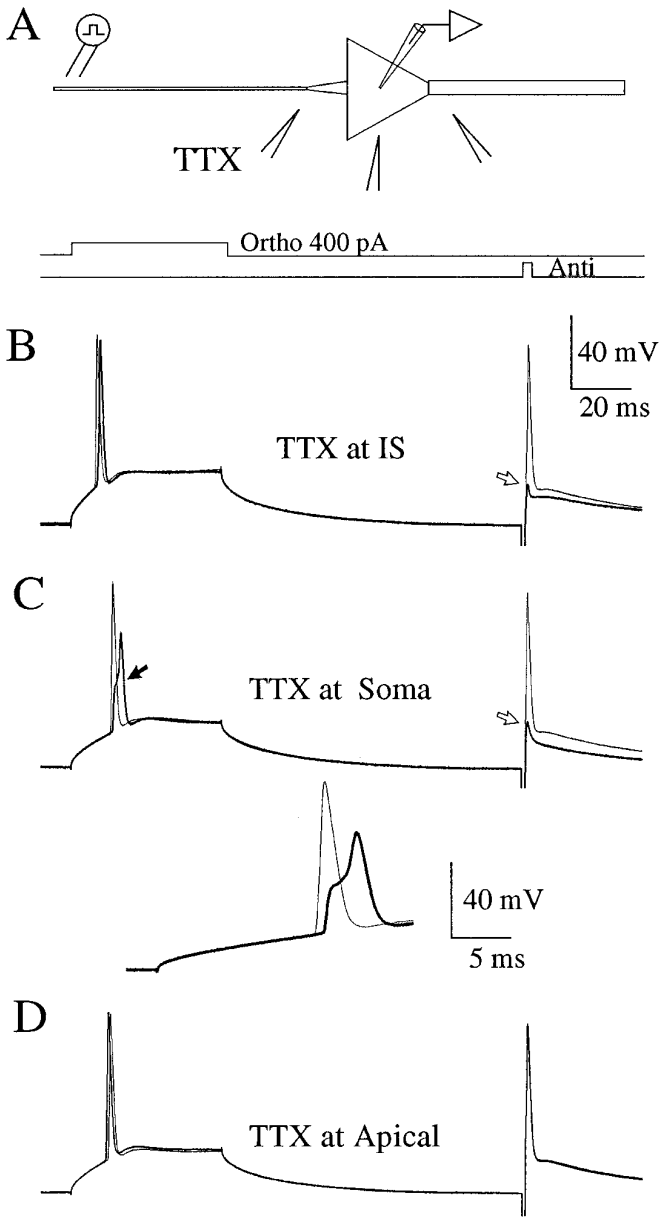

Figure 6. Local application of TTX near the soma and apical dendrite does not significantly alter the threshold for AP initiation. *A*, Experimental configuration as in Figure 5, except that the TTX pipette was placed at the initial segment (12 μm from the soma), the soma, or the apical dendrite (12 μm from the soma). In each of the *lower* panels, the *bold trace* corresponds to the presence of TTX; the *thin traces* correspond to the sweep just before the application of TTX. *B*, Local application of TTX to the initial segment caused a failure of the antidromic AP (*open arrow*), without altering the threshold to orthodromic stimuli. *C*, Local application of TTX to the soma caused a partial block of the somatic AP. *Inset* shows same sweeps at faster sweep speed. *D*, Local application of TTX to the apical dendrite had no effect on antidromic or orthodromic AP invasion of the soma. RMP, −65 mV. Cell c95094.

The results of the TTX applications taken together with the results of the dual recordings, which showed that the action potential appeared in the initial segment before the soma, point to an axonal site of initiation. Thus, we applied TTX to various positions along the axon between the soma of the pyramidal neuron and the alveus (Fig. 7*A*) while performing the same orthodromic/antidromic stimulus paradigm already described (Fig. 7*B*). The effect of TTX applied to the axon varied as a function of position. TTX applied to sites near the stimulating electrode in the alveus completely blocked the antidromic action potential (i.e., not even a partial action potential was observed) but had no effect on the orthodromic spike (data not shown). This result suggests that the antidromic action potential was blocked by raising the threshold near the stimulating electrode distal to the site of initiation for an orthodromic action potential. TTX applied at ~50 μm from the soma increased the latency and somatic membrane potential at which action potentials appeared. In two of six cells orthodromic initiation of action potentials in response to the current step was prevented altogether (Fig. 7*B,C*). The effect was rapidly reversible with action-potential initiation returning to baseline within seconds (Fig. 7*B, bottom panel*). During this shift in the apparent threshold at the soma, there was no readily observable change in the antidromic action potential in four of six cells (Fig. 7*B*). In two cells, however, there was an increase in the latency of the antidromic action potential (Fig. 7*D*). This result can be explained by the TTX application reducing the safety factor in the axon some distance from the soma. As the antidromic action potential propagated through the affected region, it slowed or even began to fall. Once beyond this region, however, the action potential regained its normal shape and invaded the soma, as in the control condition. Thus, all that was observed at the soma was a change in latency. No differences in these results were found between adult or pup slices or between room temperature and 31–32°C ($n = 3$).

Although the extent of the spread of TTX could not be monitored directly, which ultimately limited the resolution of this technique, the physiological effects of TTX application at the soma and at the initial segment (~10 μm from the soma) provided useful controls for the effects of TTX application to the axon (~50 μm from the axon). First, as shown above, TTX applied to the initial segment blocked somatic invasion of antidromic action potentials without significantly changing the orthodromic threshold. Thus, the increased orthodromic threshold observed when TTX was applied to the axon could not be explained simply by diffusion of TTX to the soma or to the initial segment. Second, TTX applied to the axon, sufficient to raise the orthodromic threshold nearly 10 mV, did not block the somatic invasion of antidromic action potentials (compare Fig. 7*C,D*). Using these physiological checks on the spread of TTX, we observed the effect of TTX application on orthodromic action-potential threshold as a function of distance from the soma. To ensure adequate delivery of TTX at positions 10 and 20 μm from the soma, we required a failure of somatic invasion of the antidromic action potential (compare Fig. 5*B*). To control for the spread of TTX to the initial segment from more distal positions (>20 μm from the soma), we required that the TTX application not cause any failure or decrease in the amplitude or latency of the somatic invasion of the antidromic action potential. If these conditions were not met, we waited for recovery and repeated the application of TTX. The effect of TTX on the apparent somatic threshold was greatest (~8 mV) when TTX was applied at distances 30–60 μm from the soma (Fig. 8; $n = 8$ cells), suggesting that the initiation of

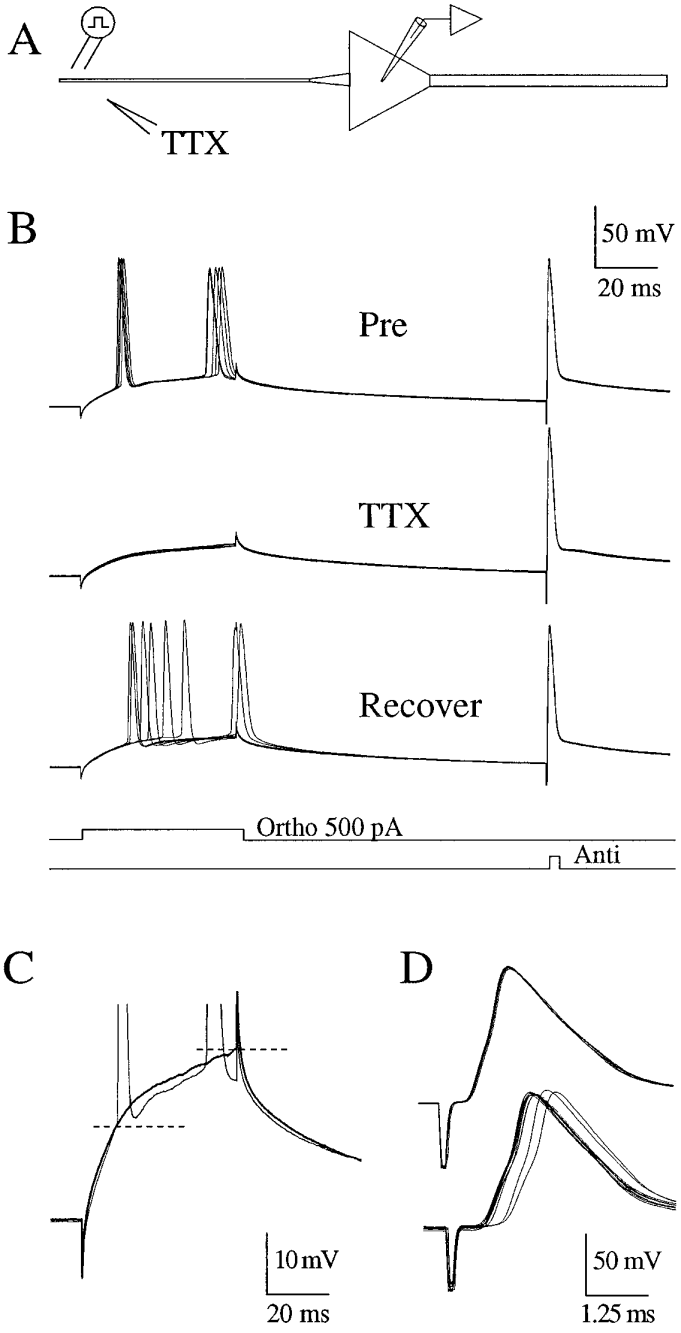

Figure 7. Local application of TTX to the axon alters the threshold for orthodromic AP initiation. *A*, Experimental configuration as in Figure 5, except that the TTX pipette was placed near the axon 50 μm from the soma. In each sweep a 500 pA current step through the recording electrode was followed by an antidromic stimulus in the alveus. *B, Pre*, Five consecutive sweeps before the application of TTX. *TTX*, Five consecutive sweeps after TTX was applied to the axon. *Recover*, Six consecutive sweeps during the recovery from the TTX application. Note that the antidromic AP was not altered by the TTX application. *C*, Single sweeps from *B* for comparison at increased gain. Application of TTX on the axon increased the apparent threshold for orthodromic AP initiation by at least 10 mV (*bold trace*). RMP, −61. Cell c95090. *D*, In another cell, application of TTX to the axon (60 μm from soma) increased the latency of the antidromic action potential. Threshold for the orthodromic AP increased by >10 mV (data not shown). RMP, −63 mV. Cell c95082.

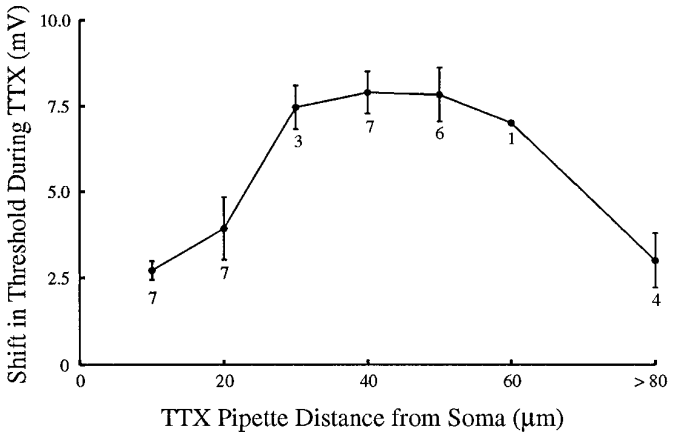

Figure 8. Shift in threshold for orthodromic action-potential (AP) initiation as a function of the location of TTX application. Experimental configuration is the same as in Figure 7. To control for the spread of TTX and to ensure adequate delivery, TTX ejections at locations 10 and 20 μm from the soma were required to be sufficient to block somatic invasion of the antidromic AP, as in Figure 5. TTX ejections beyond 20 μm were required not to block somatic invasion of the antidromic AP. The most effective locations of TTX application seem to be in the axon beyond the initial segment. Error bars are SEM. *Numbers* under each *point* are the number of neurons tested with TTX at that distance from the soma.

orthodromic action potentials depended critically on the excitability of this region of the axon.

DISCUSSION

The present data support a picture of action-potential initiation similar to the classical scheme derived from the work of Eccles and colleagues in the motoneuron (Coombs et al., 1957) yet quite different in some important details. Consistent with the motoneuron findings, action potentials initiate in the axon at a lower membrane potential than in the soma. However, in contrast to the conclusions of Eccles and colleagues, the present data suggest that the site of initiation is in the axon beyond the end of the initial segment and that the thresholds in the axon hillock and in the initial segment (for at least most of its length) are similar to that of the somatic membrane. Moreover, the present findings are inconsistent with the classic hypothesis of a very high local density of Na^+ channels in the axon hillock and initial segment (Dodge and Cooley, 1973).

Estimates of Na^+ channel density

Estimates of Na^+ channel density from cell-attached patch recordings from somata agree well with other recent studies estimating channel density with similar techniques (Stuart and Sakmann, 1994; Magee and Johnston, 1995), and slightly lower than estimates derived from dissociated somata (Sah et al., 1988; Cummins et al., 1994). Assumptions in estimating the actual density of channels from current density measurements include the area of the patch, the probability of opening, the number of activatable channels, and uniformity of density in the membrane (i.e., no clustering). The greatest potential sources of error in these measurements at present seem to be the estimate of the area of the patch attributable to stretching of the membrane. Such errors might confound the results if they are of different magnitudes in somatic and initial segment patches, because our conclusions are based on a relative measure of the densities. As an absolute measure of the density of channels, it would not be surprising if we underestimated the density by two- to threefold.

Estimates using other techniques have found evidence for a greater density of Na^+ channels in the initial segment than in the soma, although quantitative measures by each of these techniques is difficult. A study using fluophore-labeled Na^+ channel toxins and confocal microscopy (with resolution ~1 μm), estimated a fourfold, but sometimes up to a 30-fold, greater labeling of the initial segment of cultured spinal cord neurons (Angelides et al., 1988). Cortical neurons in the same study showed a less obvious increase. A study of retinal ganglion cells (requiring permeabilization of the cells for visualization) estimated a sevenfold increase in density in the initial segment (Wollner and Catterall, 1986). Finally, a freeze fracture study in frog dorsal root ganglion cells found particle counts (not necessarily Na^+ channels) to be threefold higher in the initial segment than in the soma (Matsumoto and Rosenbluth, 1985). These results suggest that the density of Na^+ channels may be higher in the initial segment in some cell types. None of these results, however, supports the conjecture that the density of Na^+ channels may approach that in a node of Ranvier (Dodge and Cooley, 1973; Mainen et al., 1995). Recent estimates of nodal densities are on the order of 1000–2000 channels/μm^2 (Black et al., 1990), as compared with 3–4 channels/μm^2 estimated in initial segments in the present study.

Local thresholds and site of initiation of action potentials

Despite the conclusion carried forth that the axon hillock/initial segment was the site of action-potential initiation, Coombs et al. (1957) noted the possibility that action potentials might instead initiate in the axon, perhaps at the first node of Ranvier. Their experiments could not distinguish between these sites because of the very short latencies involved. The site of initiation in the stretch receptor was found, using different approaches, to be in the axon beyond the initial segment (Edwards and Ottoson, 1958). Gogan et al. (1983) have argued that the electrotonic length of the initial segment of the motoneuron is relatively short. Thus, the first node of Ranvier should be depolarized essentially to the same degree as the soma. If the threshold of the initial segment, say attributable to equivalent Na^+ channel density, were similar to that of the soma, the first node would likely be the site of initiation in the motoneuron. The present experiment, that TTX applied to the axon raises the apparent threshold in the soma, seems consistent with initiation of orthodromic action potentials at the first node. However, similar results might also be expected without invoking the presence of a node if the axon had a lower threshold, in general, than the remainder of the neuron. A lower threshold could be attributable to uniformly higher density of Na^+ channels or to small diameter. Whether the Na^+ channel density in the axon beyond the initial segment is higher than that in the soma remains to be determined. With the present technique, such measurements will be limited to larger cells. The small diameter (<0.75 μm) of the axon beyond the initial segment of the subicular pyramids precludes more distal measurements.

The present experiments leave open the possibility that action-potential initiation occurs at a heminode at the very end of the initial segment. Although we observed no great differences in current in 27 patches throughout the extent of the initial segment, if a small region at the end of the initial segment had a high density of Na^+ channels, then it is possible that we missed this high density because of sampling error. Nonetheless, we found no evidence for the hypothesis that the axon hillock/initial segment is a region of uniformly high density that determines action-potential initiation. Likewise, although the most effective location

of TTX application seems to be well beyond the end of the initial segment, we cannot completely exclude the possibility that the shift in threshold is attributable to an effect of TTX at the most distal region of the initial segment. If spread of TTX to the distal initial segment explained the shift in threshold, then the idea that initiation occurs in the initial segment would, in some sense, be salvaged. This would be a somewhat semantic argument, however, because the axon hillock and most of the initial segment would still not provide the classically hypothesized function of action potential initiation but rather, as we advocate here, electrical isolation of the initiation zone from the soma modulated by axoaxonic synapses (see below).

Function of the initial segment

The focus on the initial segment as the site of action-potential initiation has overshadowed other potential functions of this region. First, one well known feature of the initial segment is the presence of axoaxonic GABA-mediated synapses, which have been hypothesized to alter the initiation of action potentials (Palay et al., 1968; Peters et al., 1968; Fariñas and DeFelipe, 1991; Cobb et al., 1995). Such synapses would likely be particularly effective in inhibiting action-potential initiation if the site of initiation were beyond the initial segment. In such a configuration, the initial segment would provide some electrical isolation between the soma–dendrites and the usual site of initiation. Thus, the soma would not need to be discharged fully by the inhibitory synapses to hyperpolarize the site of initiation away from threshold. Second, a less well known feature of the initial segment is a cisternal organelle, similar in morphology to a spine apparatus, which is thought to be involved in the sequestration of Ca^{2+} and to be coupled to the GABAergic synapses (Benedeczky et al., 1994). Although no function for this cistern has been demonstrated, the initial segment may be involved in the regulation of Ca^{2+}-dependent processes, particularly related to repetitive firing (Lüscher et al., 1996). Third, when action potentials initiate in the axon, they propagate back into the soma. For such backpropagation to succeed, the initial segment must provide enough current to charge the capacitance of the soma sufficiently to activate somatic Na^+ channels. Thus, depending on the morphology of the cell, particularly the relative diameters of the initial segment and the soma, an increased density of Na^+ channels may be needed to provide this current, without necessarily being related to producing a low threshold for action-potential initiation.

The present study only considered current injection into the soma as the orthodromic stimulus. This does not preclude initiation of action potentials in the dendrites under certain patterns of synaptic input. The present result that the threshold in the soma and earlier results (Stuart and Sakmann, 1994) that the threshold in the dendrites is at least 10 mV higher than the axonal threshold suggest that the neuron is biased toward initiation of action potentials in the axon. However, axoaxonic synapses and other specializations of the initial segment may alter the relative depolarization between the axon and the soma–dendrites, thus removing this bias and allowing the dendrites to initiate action potentials. Further work will be necessary to determine how synaptic input to the initial segment modifies thresholds and possibly the location of action-potential initiation.

REFERENCES

Adams PR (1992) The platonic neuron gets the hots. Curr Biol 2:625–627.

Angelides KJ, Elmer LW, Loftus D, Elson E (1988) Distribution and lateral mobility of voltage-dependent sodium channels in neurons. J Cell Biol 106:1911–1924.

Araki T, Otani T (1955) Response of single motoneurons to direct stimulation in toad's spinal cord. J Neurophysiol 18:472–485.

Benedeczky I, Molnár E, Somogyi P (1994) The cisternal organelle as a Ca^{2+}-storing compartment associated with GABAergic synapses in the axon initial segment of hippocampal pyramidal neurones. Exp Brain Res 101:216–230.

Black JA, Kocsis JD, Waxman SG (1990) Ion channel organization of the myelinated fiber. Trends Neurosci 13:48–54.

Cobb SR, Buhl EH, Halasy K, Paulsen O, Somogyi P (1995) Synchronization of neuronal activity in hippocampus by individual GABAergic interneurons. Nature 378:75–78.

Coombs JS, Curtis DR, Eccles JC (1957) The generation of impulses in motoneurones. J Physiol (Lond) 139:232–249.

Cummins TR, Xia Y, Haddad GG (1994) Functional properties of rat and human neocortical voltage-sensitive sodium currents. J Neurophysiol 71:1052–1064.

Dodge FA, Cooley JW (1973) Action potential of the motoneuron. IBM J Res Dev 17:219–229.

Edwards E, Ottoson D (1958) The site of impulse initiation in a nerve cell of a crustacean stretch receptor. J Physiol (Lond) 143:138–148.

Fariñas I, DeFelipe J (1991) Patterns of synaptic input on corticocortical and corticothalamic cells in the cat visual cortex. II. The axon initial segment. J Comp Neurol 304:70–77.

Fuortes MGF, Frank K, Becker MC (1957) Steps in the production of motoneuron spikes. J Gen Physiol 40:735–752.

Gogan P, Gueritaud JP, Tyc-Dumont S (1983) Comparison of antidromic and orthodromic action potentials of identified motor axons in the cat's brain stem. J Physiol (Lond) 335:205–220.

Häusser M, Stuart G, Racca C, Sakmann B (1995) Axonal initiation and active dendritic propagation of action potentials in substantia nigra neurons. Neuron 15:637–647.

Horikawa K, Armstrong WE (1988) A versatile means of intracellular labelling: injection of biocytin and its detection with avidin conjugates. J Neurosci Methods 25:1–11.

Jaffe DB, Johnston D, Lasser-Ross N, Lisman JE, Miyakawa H, Ross WN (1992) The spread of Na^+ spikes determines the pattern of dendritic Ca^{2+} entry into hippocampal neurons. Nature 357:244–246.

Jaslove SW (1992) The integrative properties of spiny distal dendrites. Neuroscience 47:495–519.

Johnston D, Magee JC, Colbert CM, Christie BR (1996) Active properties of neuronal dendrites. Annu Rev Neurosci 19:165–186.

King MA, Louis PM, Hunter BE, Walker DW (1989) Biocytin: a versatile anterograde neuroanatomical tract-tracing alternative. Brain Res 497:361–367.

Levy WB, Colbert CM, Desmond NL (1990) Elemental adaptive processes of neurons and synapses: a statistical/computational perspective. In: Neuroscience and connectionist theory (MGluck, Drumelhart, eds), pp 187–235. Hillsdale, NJ: Erlbaum.

Lüscher C, Lipp P, Lüscher H-R, Niggli E (1996) Control of action potential propagation by intracellular Ca^{2+} in cultured rat dorsal root ganglion cells. J Physiol (Lond), in press.

Magee JC, Johnston D (1995a) Synaptic activation of voltage-gated channels in the dendrites of hippocampal pyramidal neurons. Science 268:301–304.

Magee JC, Johnston D (1995b) Characterization of single voltage-gated Na^+ and Ca^{2+} channels in apical dendrites of rat CA1 pyramidal neurons. J Physiol (Lond) 487:67–90.

Mainen ZF, Joerges J, Huguenard JR, Sejnowski TJ (1995) A model of spike initiation in neocortical pyramidal neurons. Neuron 15:1427–1439.

Matsumoto E, Rosenbluth J (1985) Plasma membrane structure at the axon hillock, initial segment, and cell body of frog dorsal root ganglion cells. J Neurocytol 14:731–747.

Moore JW, Stockbridge N, Westerfield M (1983) On the site of impulse generation in a neurone. J Physiol (Lond) 336:301–311.

Palay SL, Sotelo C, Peters A, Orkland PM (1968) The axon hillock and the initial segment. J Cell Biol 38:193–201.

Peters A, Proskauer CC, Kaiserman-Abramof IR (1968) The small pyramidal neuron of the rat cerebral cortex: the axon hillock and the initial segment. J Cell Biol 39:604–619.

Sah P, Gibb AJ, Gage PW (1988) The sodium current underlying action potentials in guinea pig hippocampal CA1 neurons. J Gen Physiol 91:373–398.

Shadlen MN, Newsome WT (1994) Noise, neural codes, and cortical organization. Curr Opin Neurobiol 4:569–579.

Softky WR, Koch C (1993) The highly irregular firing of cortical cells is inconsistent with temporal integration of random EPSPs. Neuroscience 13:334–350.

Somogyi P, Freund TF, Cowey A (1982) The axo-axonic interneuron in the cerebral cortex of the rat, cat, and monkey. Neuroscience 7:2577–2607.

Spruston N, Schiller Y, Stuart G, Sakmann B (1995) Activity-dependent action potential invasion and calcium influx into hippocampal CA1 dendrites. Science 268:297–300.

Stuart GJ, Sakmann B (1994) Active propagation of somatic action potentials into neocortical pyramidal cell dendrites. Nature 367:69–72.

Stuart GJ, Dodt HU, Sakmann B (1993) Patch-clamp recordings from the soma and dendrites of neurones in brain slices using infrared video microscopy. Pflügers Arch 423:511–518.

Traub RD, Jefferys JGR, Miles R, Whittington MA, Tóth K (1994) A branching dendritic model of a rodent CA3 pyramidal neurone. J Physiol (Lond) 481:79–95.

Turner RW, Meyers DER, Richardson TL, Barker JL (1991) The site for initiation of action potential discharge over the somatodendritic axis of rat hippocampal CA1 pyramidal neurons. J Neurosci 11:2270–2280.

Wollner DA, Catterall WA (1986) Localization of sodium channels in axon hillocks and initial segments of retinal ganglion cells. Proc Natl Acad Sci USA 83:8424–8428.